united nations
ucational, scientific
and cultural
organization

ternational atomic
energy agency

the
abdus salam
international centre for theoretical physics

H4.SMR/1150 - 29

Fifth Workshop on Non-Linear Dynamics
and Earthquake Prediction

4 - 22 October 1999

Colliding Cascades as a Model for Earthquake Prediction

(Preprint)

V. Keilis-Borok

International Institute of Earthquake Prediction
Theory and Mathematical Geophysics
Russian Academy of Sciences
Moscow 113556, Russian Federation

COLLIDING CASCADES AS A MODEL FOR EARTHQUAKES PREDICTION

Gabrielov, A.M.[1], Keilis- Borok, V.I.[2], Zaliapin, I.V.[2] and Newman, W.I.[3]

[1] - Department of Earth and Atmospheric Sciense, Purdue University,W.Lafayette, IN47907-1395, USA

[2] - International Institute of Earthquake Prediction Theory and Mathematical Geophysics, Russian Academy of Science, Moscow, Russia

[3] - Department of Earth and Space Science, Astronomy, and Mathematics, University of California, Los Angeles, CA 90024, USA

EXTENDED ABSTRACT

The model of colliding cascades was introduced in the previous paper by the same authors, "Critical transitions in colliding cascades". Seismicity generated by this model satisfies basic heuristic constraints derived from observations: seismic cycle, intermittence of seismic regime, power-law energy distribution, earthquake clustering, and a set of seismicity patterns premonitory to a strong earthquake. The latter include the three patterns established by statistically significant prediction of real (observed) earthquakes. They reflect premonitory raise of seismicity and earthquake clustering. Two more patterns reflecting premonitory increase of the range of the earthquakes' correlation are found in the model itself and remain hypothetical until tested by analysis of observations.

However the previous paper considered only *existence* of the premonitory patterns in the statistical sense: it was demonstrated that on average they emerge more frequently as a strong earthquake approaches. Here, we examine their *performance* in prediction of individual strong earthquakes, one by one.

All unexplained definitions and notations are the same as in the previous paper. It is referred to as CC1.

1. Premonitory patterns considered

We consider here three basic types of premonitory patterns. Two patterns (N and Σ) reflect seismic activity. One pattern (B or "burst of aftershocks") reflects clustering of earthquakes in space and time; and two patterns (*ROC* and *Accord*) reflect the range of correlation between the earthquakes. Each pattern was defined separately for different magnitude ranges indicated by the index m. Precursor B_m was calculated for each magnitude m from 3 to 6. Precursor N_m - for each m from 1 to 6. Σ_m was calculated for events of magnitude less than or equal to m, with m varying from 2 to 6. Precursor *ROC* corresponds to events of magnitude m=2. Finally, *Accord* uses information about all the magnitudes from 1 to 6 together. Accordingly we have a set of 17

precursors related to different hypothetical premonitory patterns as well as to different magnitude ranges. Formal definition of these patterns is given in CC1.

2. General Scheme of Prediction

The aim of prediction is to determine time periods where specific events that considered to be "major" ones will occur.

Premonitory seismicity patterns are defined on a sequence of the main shocks. However the number of aftershocks is retained for each of them. We determine from this sequence different functions $F(t)$ depicting the above characteristics of seismicity. The emergence of a premonitory pattern is recognized by condition

$$F(t) \geq C_F.$$

The threshold C_F is usually defined as a $Q\%$ percentile of the function F.

Algorithm for prediction by each single pattern is formulated as follows (Fig. 1). An alarm is declared for the time period Δ after each moment when $F(t) \geq C_F$. The alarm is terminated after a major earthquake occurs or the time Δ expires, whichever comes first. The first case is a *confirmed prediction* ("success"), the second - a *false alarm*. A *failure to predict* is the case when a major earthquake occurs outside an alarm.

Prediction procedure is illustrated in Fig. 2. Function F in that case is the weighted number of earthquakes with magnitudes from 1 to 6 in a sliding time window, $\Sigma_6(t|s)$, $s=2$. Precursor is defined by condition $\Sigma_6(t|s) \geq 0.37$. Alarm is declared for $\Delta=10$ time units. With this threshold we obtain two alarms within the considered interval. One of them is a confirmed prediction while another is a false alarm. Strong event, $m=7$, occurred at the moment $t=845.2$ indicated in the figure by an arrow.

Error diagram. As we can see from Fig.2 there is a tradeoff between confirmed predictions and errors. It depends on the adjustable parameters of a prediction algorithm. For example, raising C_Σ we would reduce the number of alarms but increase the number of failures to predict; raising Δ_Σ we will increase duration of alarms but may reduce the number of failures to predict etc. A prediction method and evaluation of its performance would make sense *only* if the success and errors score is stable to variation of adjustable parameters.

The tool for such evaluation is the error diagram introduced in the earthquake prediction research by G. Molchan (1990). Fig. 3 shows such a diagram for the precursor B_m, $m = 5$.

Prediction covers time interval T. During that interval N strong events occurred and N_f of them were missed by prediction; the number of declared alarms is A; A_f of them were false, and the total duration of alarms was D. Empty time intervals between the cycles are not counted in T. Right hand plot shows the tradeoff between relative duration of alarms $\tau = D:T$ and the rate of failures to predict $n = N_f:N$. Points on the diagonal, $n+\tau=1$, shown by bold line correspond to a random binomial prediction: the alarm is declared at each time step with probability p and not declared with probability $q = 1-p$. Left hand plot shows the tradeoff between the rate of false alarms $f = A_f:A$ and n.

Different points correspond to different thresholds C_B. Prediction with other values of m from *3* to *6* gives similar results. For advance prediction of real earthquakes the typical score is close to $n = \tau = 0.3$ or 0.4, so that such a diagram as in Fig. 3 would be quite satisfactory. Variation of other parameters of prediction algorithm, say Δ_B, may be explored in the same way; in the present study this is not necessary.

3. Performance of single precursors

Synthetic earthquake sequence where we look for precursors is the same as was analyzed in (CC1, Figs. 2 and 4). The targets of prediction are the 25 "major" earthquakes in this sequence, with magnitude $m = 7$, the strongest possible ones in the model. Premonitory patterns are formed by the earthquakes with smaller magnitudes, from 6 down to 1. Each one out of 17 considered precursors was used separately for prediction accordingly to scheme described above (section 2). Alarm was declared for Δ=10 time units.

Error diagrams for the premonitory patterns considered are given in Fig. 3-7. Again the performance is quite encouraging.

Relation to analysis of observations. Functions B_m, N_m, and Σ_m are defined here in the same way, as in the intermediate term prediction algorithms developed by analysis of observations (Keilis-Borok (ed.), 1990 and references therein). They were used for earthquake prediction in combination with other functions; Σ_m and B_m were used also independently on the other precursors. Premonitory patterns, based on these functions, are validated by statistically significant earthquake prediction (Kossobokov et al., 1999; Vorobieva, 1999). Pattern *B* is also validated independently of other ones: this is the first precursor for which statistical significance was rigorously established (Molchan et al, 1990).

Precursor *ROC* is practically identical to the one introduced by A. Prozorov (1975) for a long-term prediction of the location where a strong earthquake has to be expected. Precursor *Accord* was first introduced in the analysis of CC model (CC1).

4. Collective performance of precursors.

In the previous section we considered predictions based on the single premonitory patterns, one at a time. Each pattern was considered in different magnitude ranges also independently on each other. Here, in Figs. 8 and 9, we juxtapose the predictions by all 17 precursors considered. They are naturally divided into four groups: *B, N,* Σ, *R*.

Fig. 8 demonstrates collective performance of precursors. Top panel shows, in separate boxes, emergence of precursors before each of the 25 major earthquakes in the synthetic sequence. The right edge of each box is the moment of a major earthquake. Time interval of three units is considered before each one.

Bottom panel in Fig. 8 shows false alarms that is the alarms determined during the time periods when strong earthquakes did not occur. Vertical lines show the moments of events with $m = 6$. They are associated with most of the false alarms.

Each row in Fig. 8 shows the track record of a single precursor. Shaded areas show the alarms determined by it. Values of m indicate the magnitude range, in which a precursor is determined. Let us remind that precursors of the group N are determined separately for each magnitude. Precursors of the group Σ are determined separately for the magnitude intervals from 1 to m; and precursors B - for different magnitudes of the main shocks, which have triggered the aftershocks considered.

Fig. 9 demonstrates the collective performance of each group of precursors. Top panel indicates whether a group predicts an event or not. We regard an event as predicted by a group if it is predicted by 2 or more single precursors from this group. Shaded boxes indicate events predicted by that rule. Bottom panel shows false alarms. Again they are strongly associated with events of magnitude 6; vertical lines show the moments of these events.

Following results seem to deserve attention.

1) Predictions are not trivial even when emergence of the major earthquakes in the model follows a very simple scenario of seismic cycle.

2) Emergence of precursors is highly correlated. This is so even for precursors reflecting such different phenomena as the clustering and the rise of activity. Note in particular that the errors of predictions are also closely correlated. For example we have following persisting errors: 4 failures to predict the major earthquakes # 9, 11, 16, 24. It is suggestive that all of them situated at the end of the non-cyclical periods. Also we always have the false alarm at the beginning of these periods.
The correlation is emphasized by similarity of the error diagrams.

5. Discussion

- CC1 model is, we believe, the first one, where such a broad set of precursors is reproduced.

- The design of the model predetermines the good performance of precursors N and Σ. Precursors *Accord* and *ROC* can at least can be explained by that design. However the success of the bursts of aftershocks, B, is not predetermined at all, supporting the relevance of the model.

- CC model opens many yet untapped possibilities for earthquake prediction research. This includes: exploration of the three more types of premonitory phenomena which have been previously hypothesized - irregularity of earthquakes flow, response to excitation and decrease of dimensionality; exploration of several other precursors, such as transformation of the Gutenberg - Richter relation (Schnirman and Blanter, 1999; Rotwain et. al., 1997); more compact definition of the precursors set; prediction of earthquakes with magnitude smaller than the maximal possible one, say with $m = 6$; prediction of the changes in seismic regime (Schnirman and Blanter, 1999). Other possibilities of such kind are discussed in CC1.

Acknowledgements. This study was partly supported by the grants from the National Sciences Foundation (EAR-9804859), International Science and Technology Center (Project # 1293) and the Italian Ministry for Foreign Affairs.

References

[1] Gabrielov, A.M., Keilis-Borok, V.I., Zaliapin, I.V., Newman B.I., 1999. Critical transitions in colliding cascades. ICTP. Preprint.

[2] Molchan, G.M., 1990. Strategies in strong earthquake prediction. Phys. Earth Planet. Int. 61, 84-98.

[3] Keilis-Borok,V.I., (Ed.), 1990. Intermediate-term earthquake prediction: models, phenomenology, worldwide tests. Phys. Earth Planet. Int., 61, Special Issue, 1, 2, p.144.

[4] Kossobokov, V.G., Romashkova, L.L., Keilis-Borok, V.I. and Healy, J.H., 1999. Testing earthquake prediction algorithms: statistically significant advance prediction of the largest earthquakes in the Circum-Pacific, 1992-1997. Phys. Earth Planet. Int. 111, 187-196.

[5] Vorobieva, I.A., 1999 Prediction of a subsequent large earthquake. Phys. Earth Planet. Int. 111, 197-206.

[6] Molchan, G.M., Dmitirieva, O.E., Rotwain, I.M., Dewey, J., 1990. Statistical analysis of the results of earthquake prediction, based on bursts of aftershocks. Phys. Earth Planet. Int. 61 (1-2), 128-139.

[7] Prozorov, A.G., 1975. Variations of seismic activity related to locations of strong earthquakes. Vychislitelnaya Seismologiya 8, 71-82. (In Russian)

[8] Shnirman, M.G., Blanter E.M., 1999. Mixed hierarchical model of seismicity: scaling and prediction. Phys. Earth Planet. Int. 111, 295-303.

[9] Rotwain, I.M., Keilis-Borok, V.I., Botvina, L., 1997. Hierarchical fracturing of steel samples and premonitory transformation of earthquake flow. Phys. Earth Planet. Int. 101, 61-71.

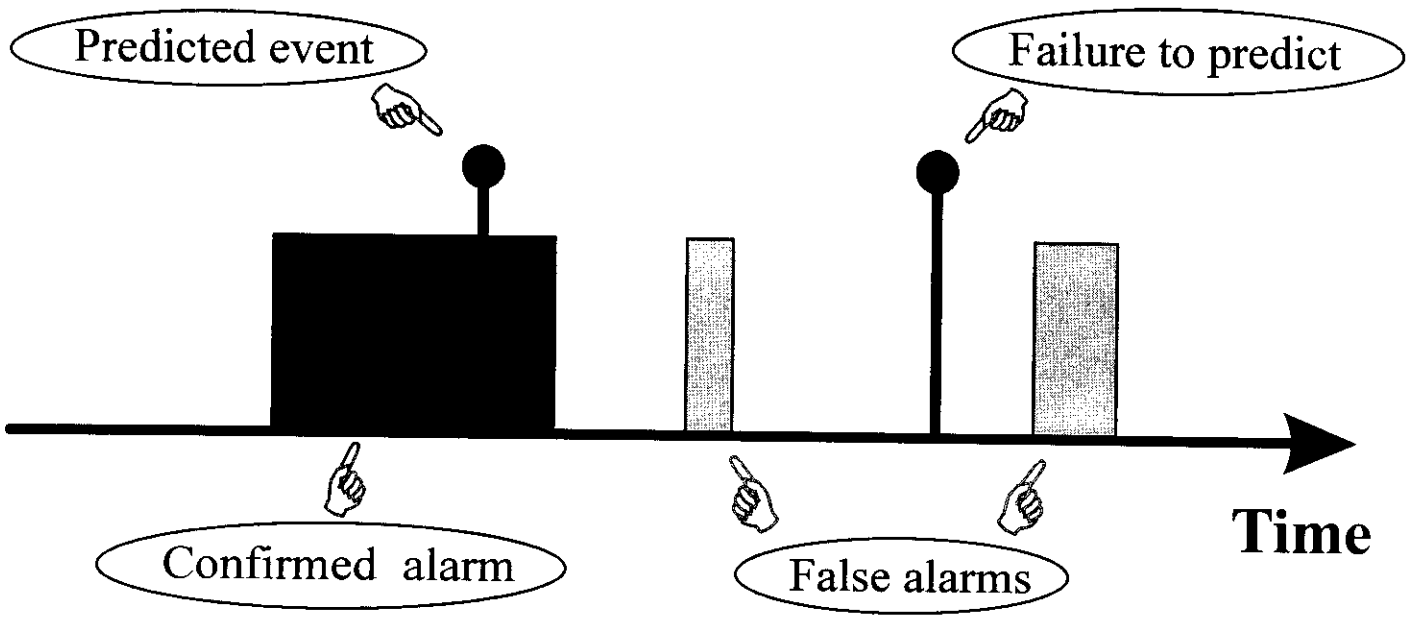

Fig. 1. Outcomes of predictions.

A.Gabrielov agabriel@ math.purdue.edu V.Keilis-Borok vkborok@mitp.ru
W.Newman win@ucla.edu I.Zaliapin zaliapin@mitp.ru

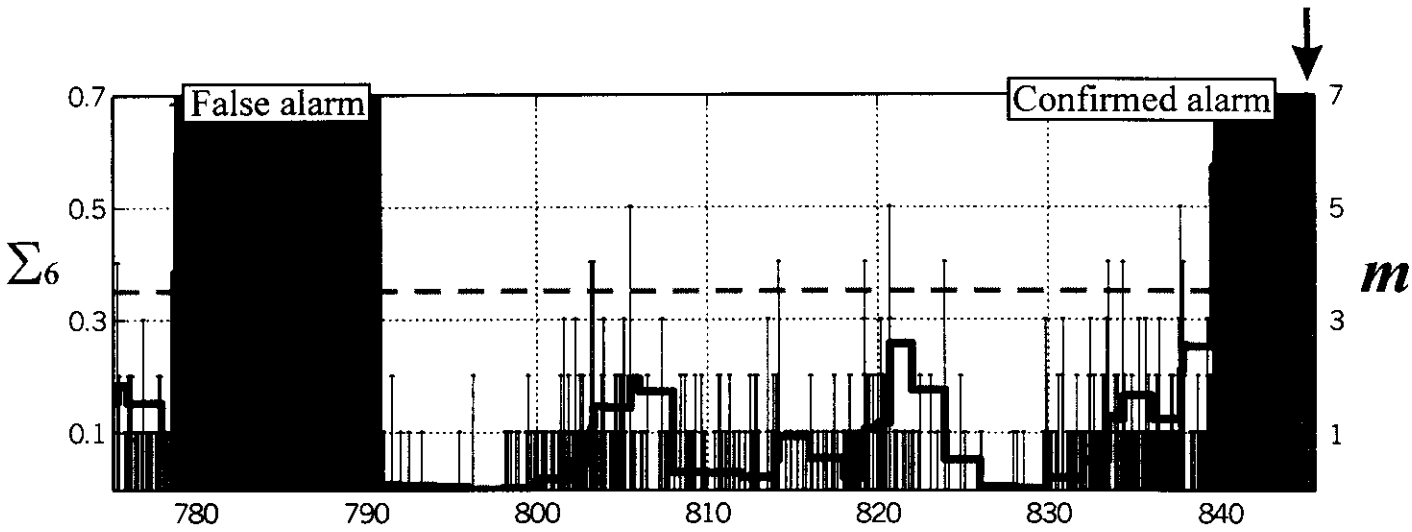

Fig. 2. Identification of precursor.

Figure shows a case history of function $\Sigma_6(t)$ during 70 time units prior to the 9-th major event (indicated by the arrow). Vertical lines - individual main shocks.

Left axis corresponds to values of Σ_6, right axis - to magnitudes m.

Dotted horizontal line is a threshold.

Alarm is declared for 10 time units when $\Sigma_6(t)$ exceeds the threshold shown by dotted line.

Dark zones mark alarms corresponding to this threshold. First is false, second - confirmed.

A.Gabrielov agabriel@ math.purdue.edu V.Keilis-Borok vkborok@mitp.ru
W.Newman win@ucla.edu I.Zaliapin zaliapin@mitp.ru

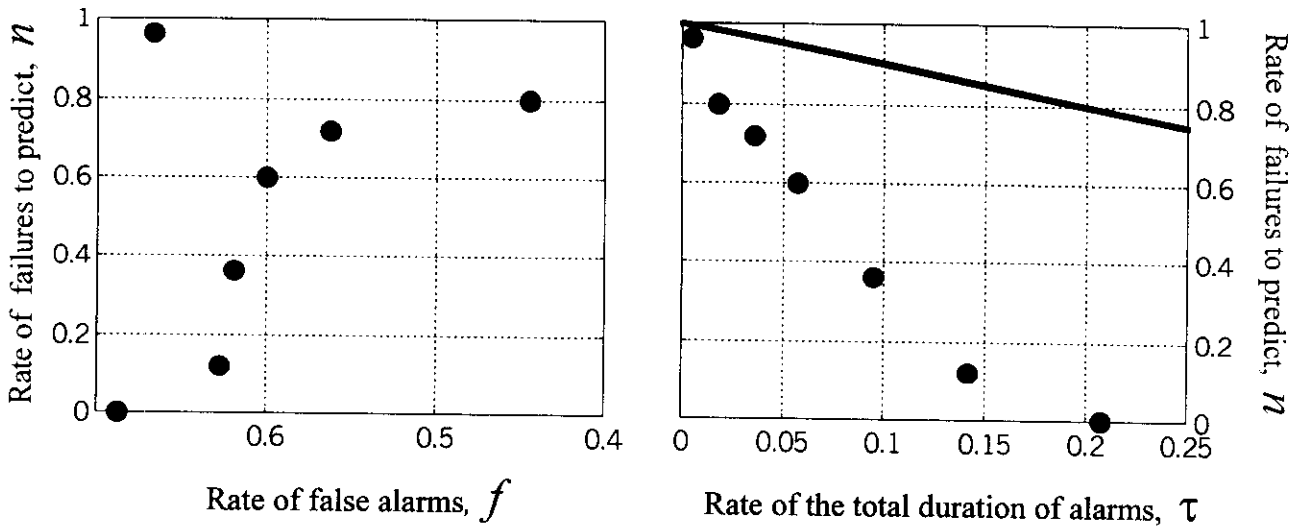

Fig. 3. Performance of prediction based on clustering (precursor "bursts of aftershocks" or B_m).

Diagrams show the tradeoff among the parameters, characterizing performance of prediction by the precursor B_5.

Prediction covers time interval T. During that interval N strong events occurred and N_f of them were missed by prediction; A alarms were declared, their total duration was D and A_f of the alarms were false ones. Empty time intervals between the cycles are not counted in T.

Right: Error diagram showing the tradeoff between relative duration of alarms $\tau = D:T$ and the rate of failures to predict $n = N_f:N$. Points on the diagonal (bold line) would correspond to a random binomial prediction.

Left: Tradeoff between the rate of false alarms $f = A_f:A$ and n.

Different points correspond to different thresholds. Prediction with other values of m from *3* to *6* gives similar results.

A.Gabrielov agabriel@ math.purdue.edu V.Keilis-Borok vkborok@mitp.ru
W.Newman win@ucla.edu I.Zaliapin zaliapin@mitp.ru

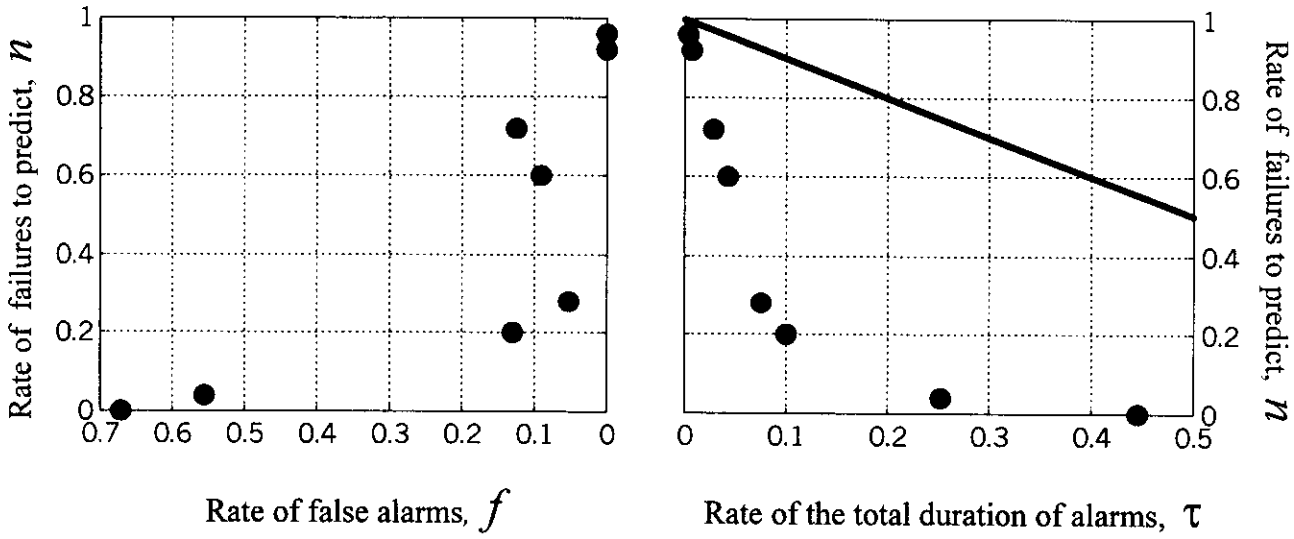

Fig. 4. Performance of prediction based on the number of main shocks (precursor N_m)

Diagrams show the tradeoff among the parameters, characterizing performance of prediction by the precursor N_2.

Prediction covered time interval T. During that interval N strong events has occurred and N_f of them were missed by prediction; A alarms were declared, their total duration was D and A_f of the alarms were false ones. Empty time intervals between the cycles are not counted in T.

Right: Error diagram showing the tradeoff between relative duration of alarms $\tau = D:T$ and the rate of failures to predict $n = N_f:N$. Points on the diagonal (bold line) would correspond to a random binomial prediction.

Left: Tradeoff between the rate of false alarms $f = A_f:A$ and n.

Different points correspond to different thresholds. Prediction with other values of m from *3* to *6* gives similar results.

A.Gabrielov agabriel@ math.purdue.edu V.Keilis-Borok vkborok@mitp.ru
W.Newman win@ucla.edu I.Zaliapin zaliapin@mitp.ru

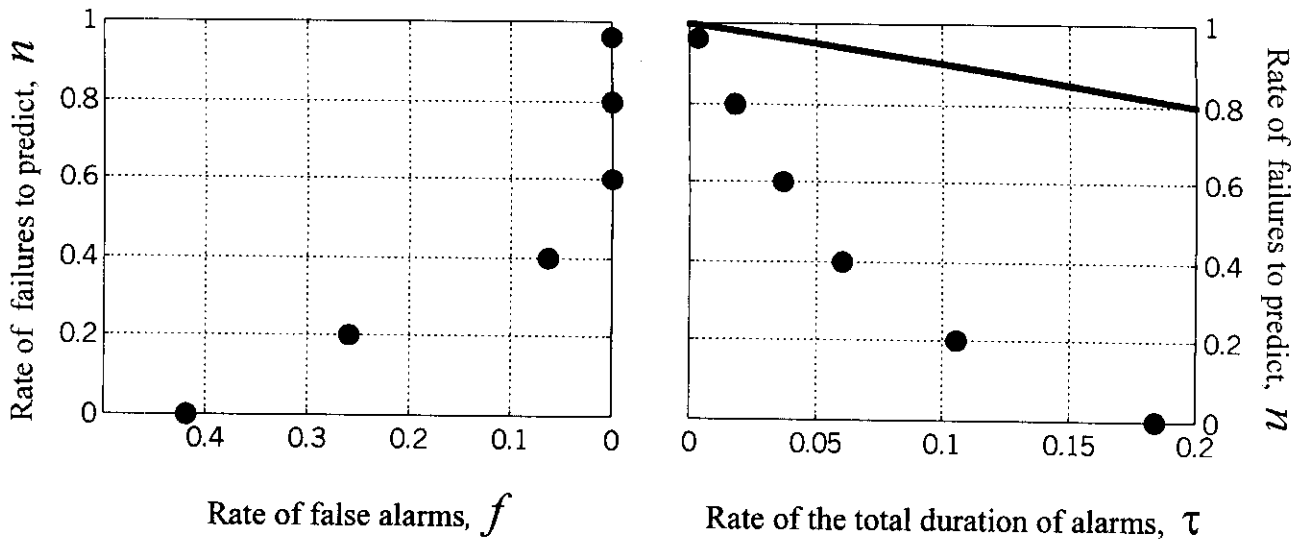

Fig. 5. Performance of prediction based on the weighted number of main shocks (precursor Σ_m).

Diagrams show the tradeoff among the parameters, characterizing performance of prediction by the precursor Σ_6.

Prediction covered time interval T. During that interval N strong events has occurred and N_f of them were missed by prediction; A alarms were declared, their total duration was D and A_f of the alarms were false ones. Empty time intervals between the cycles are not counted in T.

Right: Error diagram showing the tradeoff between relative duration of alarms $\tau = D:T$ and the rate of failures to predict $n = N_f:N$. Points on the diagonal (bold line) would correspond to a random binomial prediction.

Left: Tradeoff between the rate of false alarms $f = A_f:A$ and n.

Different points correspond to different thresholds. Prediction with other values of m from 2 to 5 gives similar results.

A.Gabrielov agabriel@ math.purdue.edu V.Keilis-Borok vkborok@mitp.ru
W.Newman win@ucla.edu I.Zaliapin zaliapin@mitp.ru

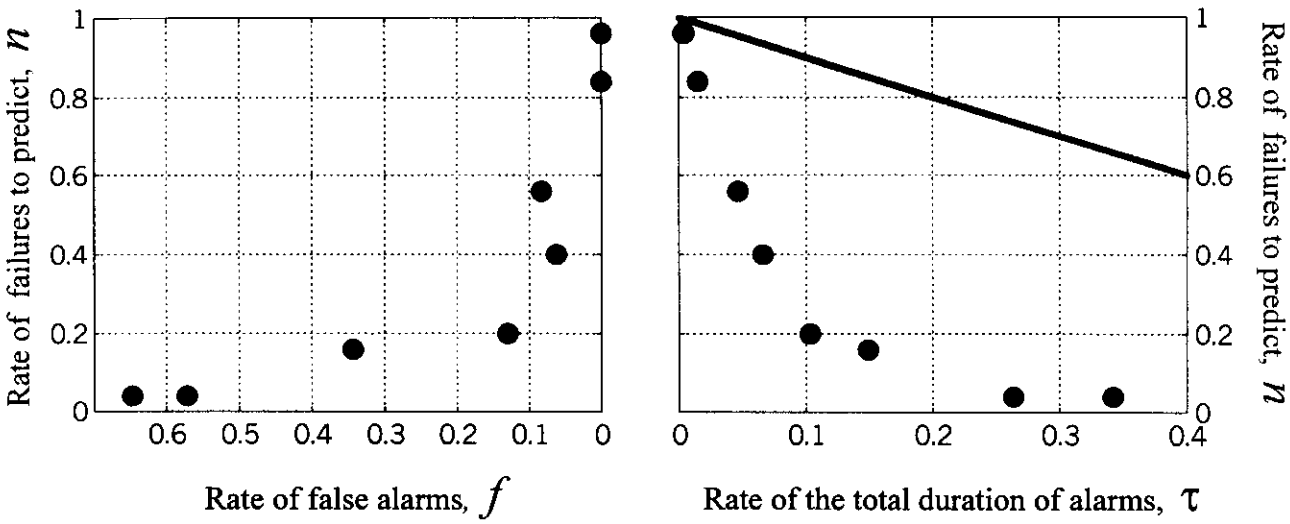

Fig. 6. Performance of prediction based on the radius of correlation (precursor *ROC*).

Diagrams show the tradeoff among the parameters, characterizing performance of prediction. Precursor was considered for main shocks of magnitude $m=2$.

Prediction covered time interval T. During that interval N strong events has occurred and N_f of them were missed by prediction; A alarms were declared, their total duration was D and A_f of the alarms were false ones. Empty time intervals between the cycles are not counted in T.

Right: Error diagram showing the tradeoff between relative duration of alarms $\tau = D:T$ and the rate of failures to predict $n = N_f:N$. Points on the diagonal (bold line) would correspond to a random binomial prediction.

Left: Tradeoff between the rate of false alarms $f = A_f:A$ and n.

Different points correspond to different thresholds.

A.Gabrielov agabriel@ math.purdue.edu V.Keilis-Borok vkborok@mitp.ru
W.Newman win@ucla.edu I.Zaliapin zaliapin@mitp.ru

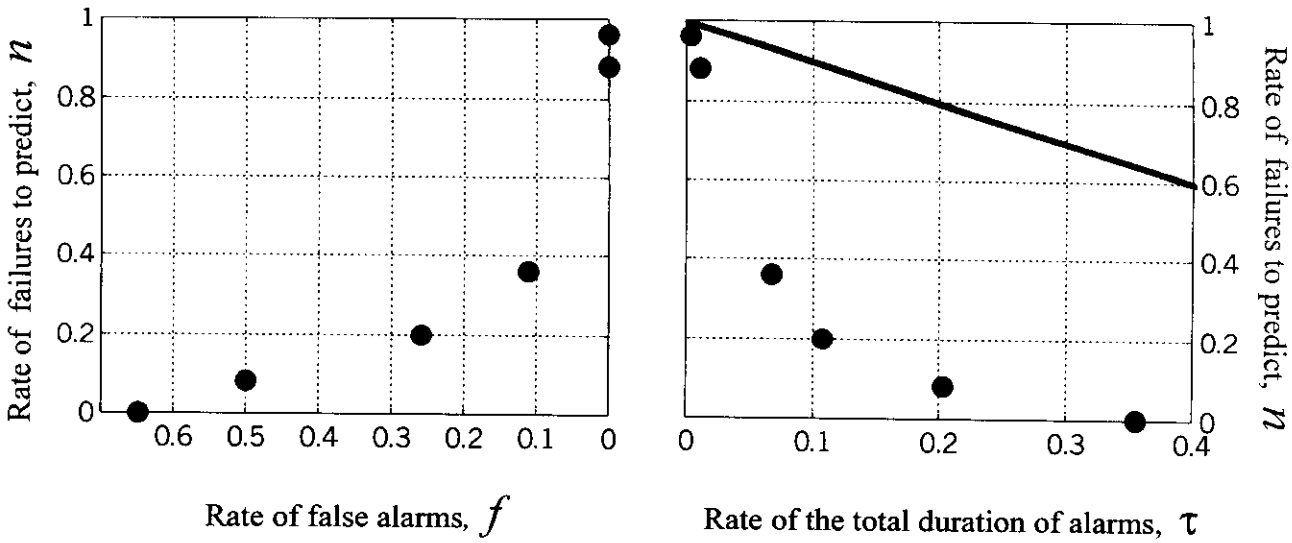

Fig. 7. Performance of prediction based on the radius of correlation (precursor *Accord*).

Diagrams show the tradeoff among the parameters, characterizing performance of a prediction algorithm.

Prediction covered time interval T. During that interval N strong events has occurred and N_f of them were missed by prediction; A alarms were declared, their total duration was D and A_f of the alarms were false ones. Empty time intervals between the cycles are not counted in T.

Right: Error diagram showing the tradeoff between relative duration of alarms $\tau = D:T$ and the rate of failures to predict $n = N_f:N$. Points on the diagonal (bold line) would correspond to a random binomial prediction.

Left: Tradeoff between the rate of false alarms $f = A_f:A$ and n.

Different points correspond to different thresholds.

A.Gabrielov agabriel@ math.purdue.edu V.Keilis-Borok vkborok@mitp.ru
W.Newman win@ucla.edu I.Zaliapin zaliapin@mitp.ru

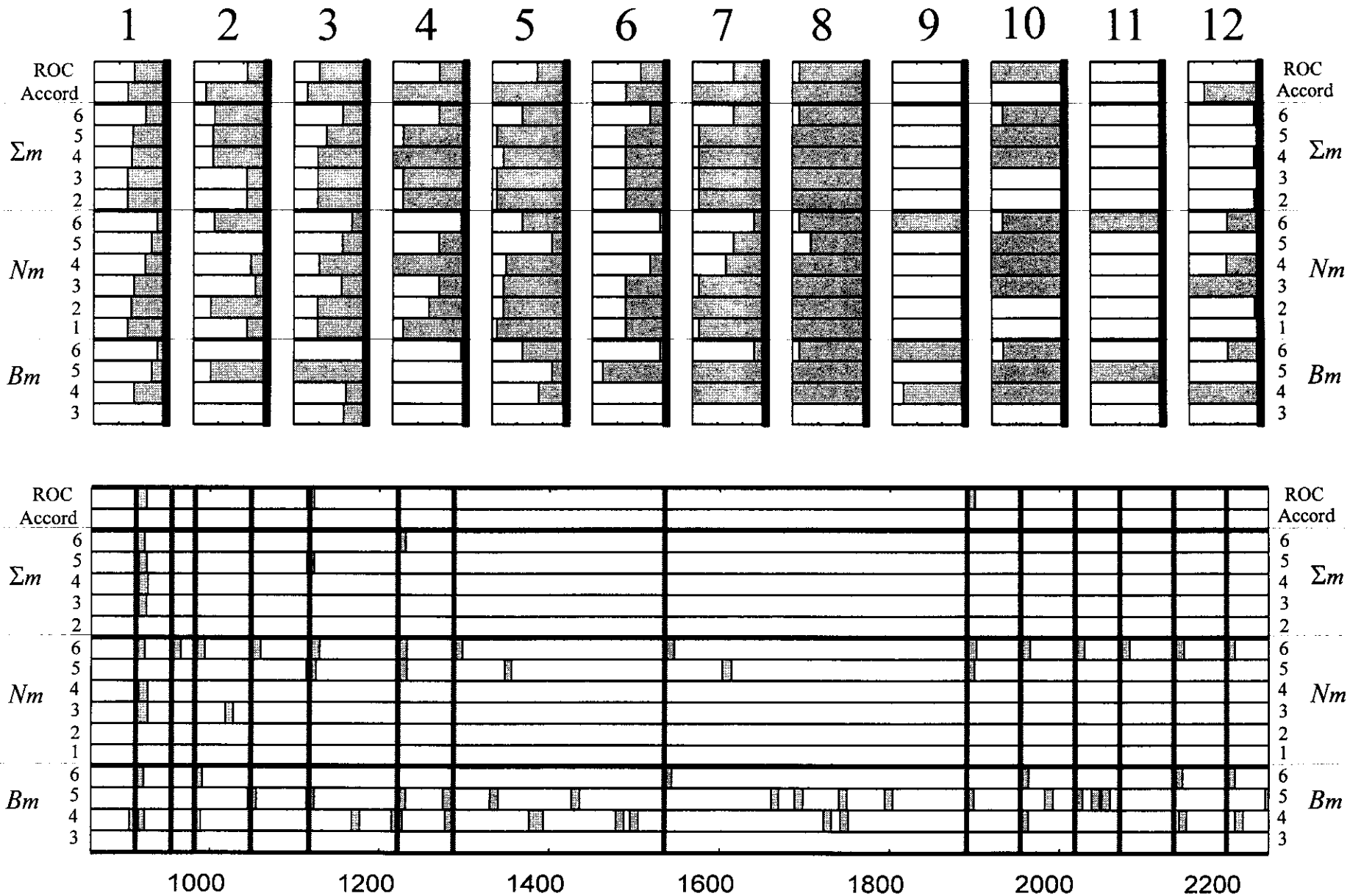

Fig. 8. Collective performance of the precursors.
***Top* - prior to each strong earthquake; *bottom* - at the time when strong events did not occur.**

A.Gabrielov agabriel@ math.purdue.edu V.Keilis-Borok vkborok@mitp.ru
W.Newman win@ucla.edu I.Zaliapin zaliapin@mitp.ru

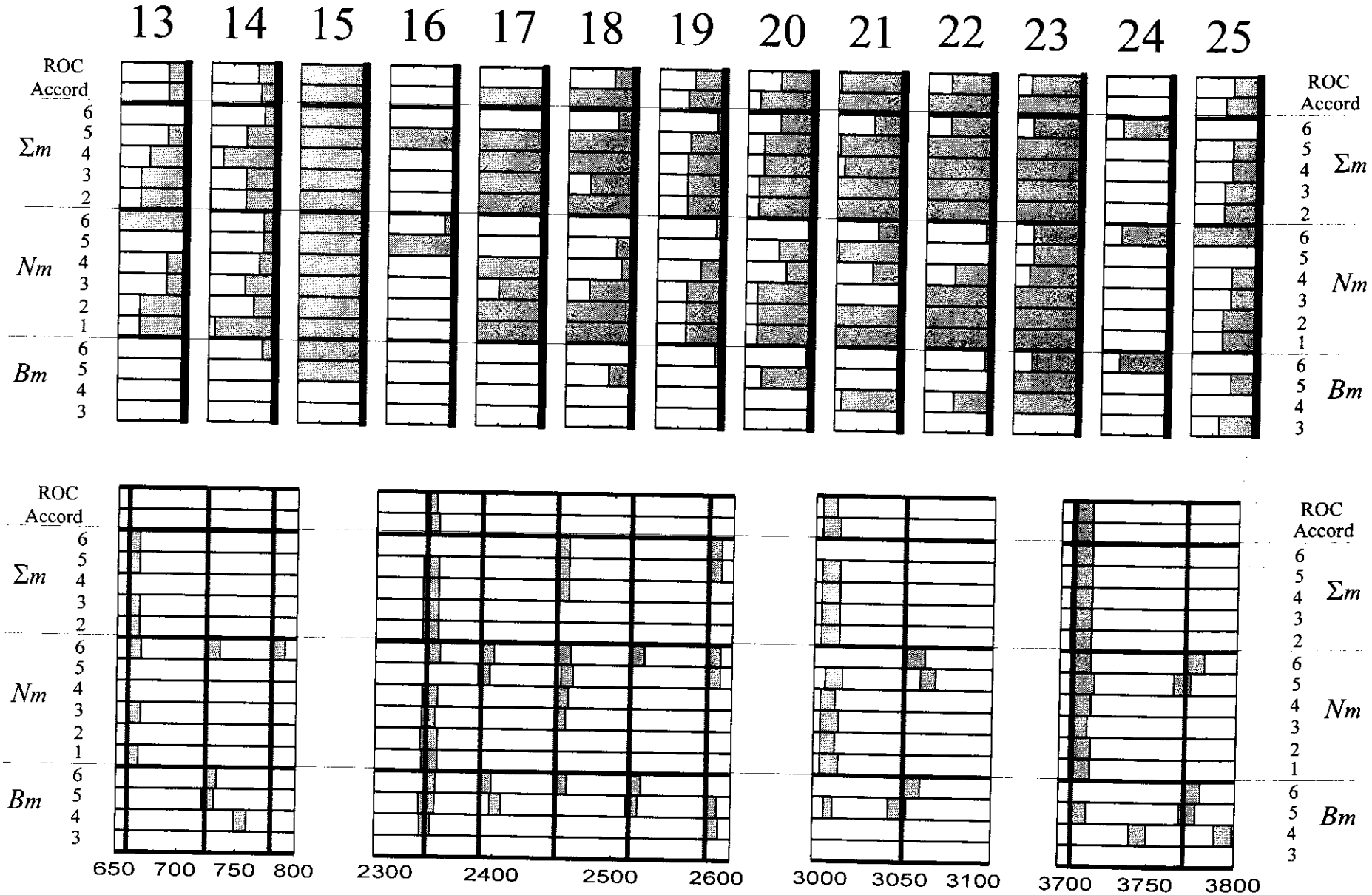

Fig. 8 (continued).

A.Gabrielov agabriel@ math.purdue.edu V.Keilis-Borok vkborok@mitp.ru
W.Newman win@ucla.edu I.Zaliapin zaliapin@mitp.ru

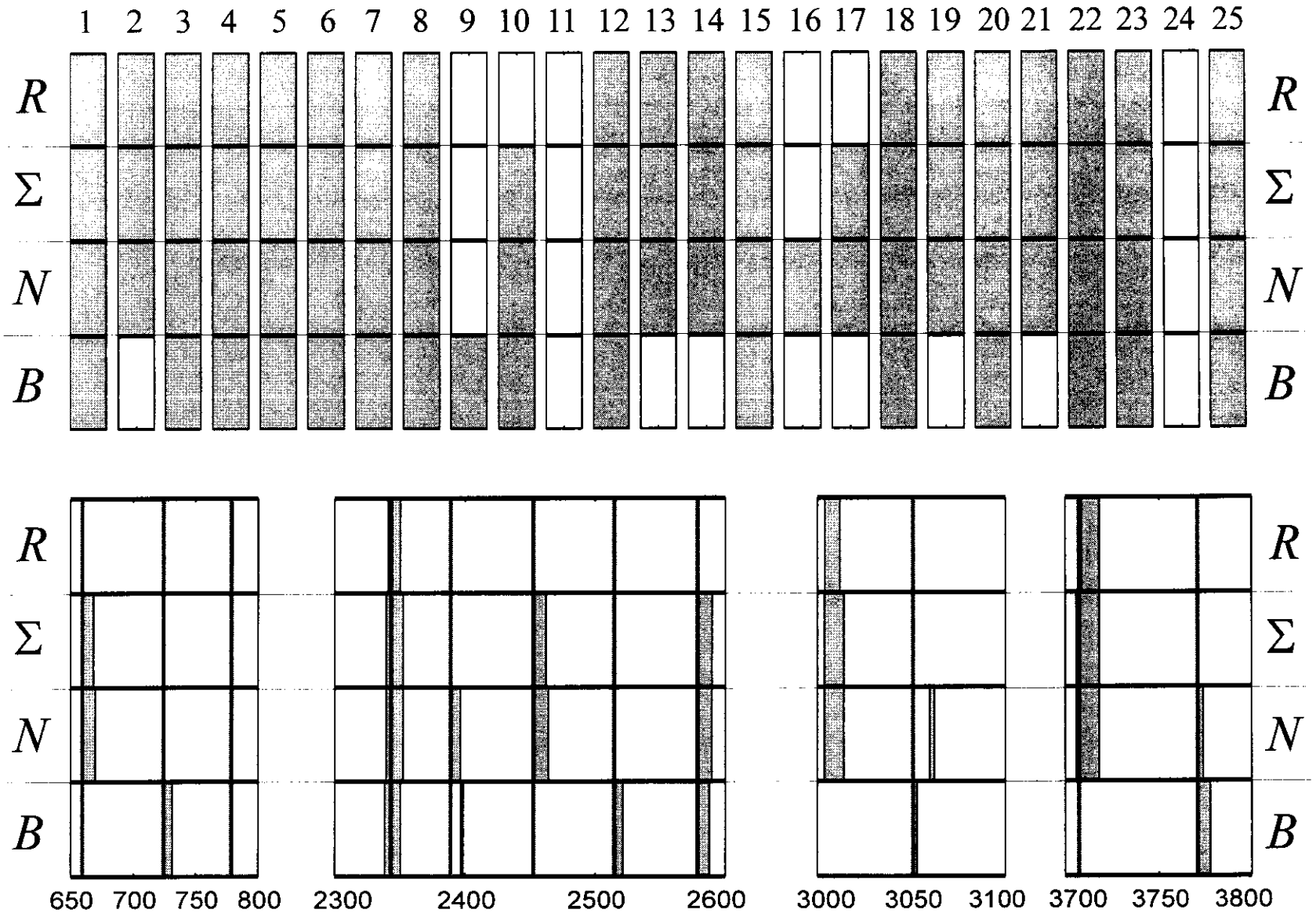

Fig. 9. Collective performance of 5 different groups of precursors.

A.Gabrielov agabriel@ math.purdue.edu V.Keilis-Borok vkborok@mitp.ru
W.Newman win@ucla.edu I.Zaliapin zaliapin@mitp.ru